MODEL A DYNAMICS AND THE DECONFINING PHASE TRANSITION
LeiLat Seminar

Bernd Berg, Florida State University

June 2004

- Lattice gauge theory investigations of the deconfining phase transition have mainly been limited to equilibrium studies.
- In nature deconfining transitions are governed by temperature and/or expansion driven dynamics
  - Early universe: slow cooling process $(10^{-5} - 10^{-6} >> 10^{-23} s)$.
  - Heavy ion collisions:
    - cooling is of the order of some relaxation time scale estimates $(5 - 10 fm/c)$;
    - rapid heating (quench) $(1 fm/c)$;

Heavy Ion Collisions

The standard picture of heavy ion collisions (Anishetty, Koehler, McLerran (1980) and Bjorken (1983)).

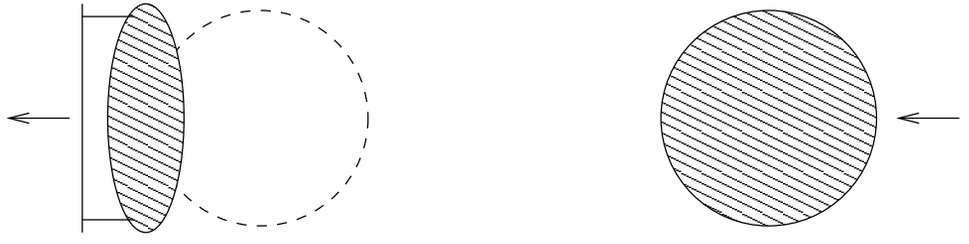

Figure 1: Central collision of heavy ions followed by formation of fireballs (target rest frame).

The projectile fragments outside the target.
Most of the baryon number is in the fragmentation region.
The target becomes compressed to an ellipse moving along the longitudinal axes.
Central rapidity region: Heated plasma of zero baryon number.

Bjorken Hydrodynamical Model for the Central Region

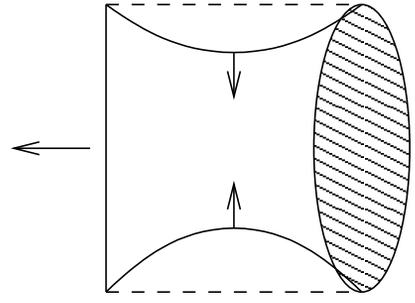

Figure 2: Fire-tunnel evolution.

The rarefraction front is formed at distances $\sim d_{\text{nucleus}}$ and move towards the center.
At ion separation $\sim d_{\text{nucleus}}$ the amount of fluid undergoing the longitudinal expansion decreases.
The remnants of the fluid expand radially and cool rapidly.
The characteristic time of evolution is $5 - 10 fm/c$.

Equilibration?

It is conjectured that rescattering inside the central rapidity region may lead to equilibration.
If the number of rescatterings needed is ~ 1, then typical times of equilibration are:

$$\tau_g \sim \frac{1}{2} fm/c \qquad \text{(gluons)} \tag{1}$$

$$\tau_q \sim 2 fm/c \qquad \text{(quarks)}\,. \tag{2}$$

This could lead to equilibration, if there were no strong dynamical effects in the vacuum of the underlying field theory.

Finite Temperature Field Theory

Based on the observation that quantum statistics formulation of a d dimensional field theory at finite T

$$Z(T,V) = \mathrm{Tr} e^{-H/T} \tag{3}$$

$$= \sum_{\phi} \langle \phi | e^{-H/T} | \phi \rangle \tag{4}$$

can be expressed as the PI representation for the transition amplitude

$$\langle \phi_1 | e^{-iHt_1} | \phi_0 \rangle = \int_{\phi_0}^{\phi_1} D\phi \, \exp[i \int_0^{t_1} d\tau L(\phi, \dot{\phi})] \tag{5}$$

$$Z(T,V) = \int_{periodic} D\phi \, \exp[- \int_0^{1/T} d\tau L_E(\phi, \dot{\phi})] \tag{6}$$

Order Parameter

For pure lattice gauge theory at finite temperature the Polyakov loop l is the confinement/deconfinement order parameter.

$$l(\vec{x}) = \mathrm{tr} \prod_{m=0}^{N_t-1} U_{\vec{x}+m\hat{t},0} \tag{7}$$

The symmetry group of the order parameter in the $SU(3)$ gauge theory is $Z(3)$.
Symmetric (confined) phase $\langle l \rangle = 0$;
Broken (deconfined) phase $\langle l \rangle \neq 0$.
The transition is weak 1st order.
Quarks smooth out this behavior. At low density the QCD transition is most likely a rapid crossover.

Dynamics

- The equilibrium theory is time-independent.
- A full non-equilibrium description (non-diagonal density matrix) causes unsurmountable technical difficulties.

Time may be reintroduced!

- Different dynamical universality classes (defined by equations of motions) may be explored.
- We study heatbath dynamics, which belongs to Model A in the material science classification (e.g. Chaikin and Lubensky, *Principles of condensed matter physics*, table 8.6.1, p.467).
- Dumitru and Pisarski (2001) add a kinetic term to an effective model of Polyakov loops $\sim |\partial_\mu l|^2$, which may then allow for simulations in Minkowski space.

The Effective Models

- LQCD, but it is difficult to simulate.
- Effective spin model for the Polyakov loops (Svetitsky and Yaffe (1982), and a lot of subsequent work)
  The 3d 3-state Potts model:

$$\mathcal{H} = -J \sum_{<ij>} \delta_{n_i,n_j} + h \sum_i \delta_{n_i,0}, \tag{8}$$

  $\beta_{\rm spin} = J/2kT$. The external magnetic field h accounts for the presence of quarks ($h \sim 1/m$).

QCD and Spin Model Temperatures

The QCD temperature T is given by

$$T = \frac{1}{N_t a(g_0)}. \tag{9}$$

For pure $SU(3)$ gluodynamics

$$a(g_0) = \frac{1}{\Lambda_L} \exp\left(-\frac{1}{2\beta_0 g_0^2}\right) = \frac{1}{\Lambda_L} \exp\left(-\frac{\beta_{\rm LGT}}{\beta_0}\right). \tag{10}$$

Therefore $\beta_{\rm LGT} \sim \beta_{\rm spin}$.

Thus T is monotonously increasing with $\beta_{\rm spin}$.

Simulated Models

- The 2D Potts models for which a number of rigorous results are known (Baxter (1973)).
- Test bed in 2D: The weak first order transition of the 5-state Potts model. Also studied: The 2-, 4-, 10-state Potts models, corresponding to a 2nd order, a "strong" 2nd order and a strong first order phase transition.
  (Berg, Heller, Meyer-Ortmanns, Veltsky, PRD 69, 034501 (2004) [hep-lat/0309130])
- The $3d$ 3-state Potts model with and without external magnetic field.
  (Berg, Meyer-Ortmanns, Veltsky, hep-lat/0405011)

Hysteresis and Quench

We study the hysteresis $\triangle\beta = \frac{2(\beta_{\max}-\beta_{\min})}{n_\beta\, L^2}$, $\triangle\beta' = \frac{2(\beta_{\max}-\beta_{\min})}{n'_\beta\, L_0^2}$, $(L_0 = 20)$, and quench dynamics $\beta = \beta_{\min} \to \beta_{\max}$.

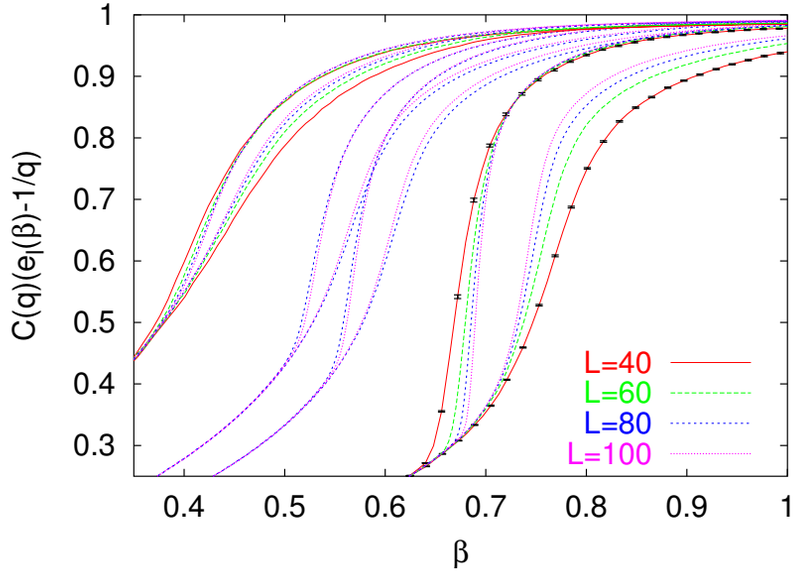

Figure 3: Rescaled energy $(C(q) = q/(q-1))$ hysteresis curves for $n_\beta = 1$ in 2d. From left to right $q = 2, 4, 5$ and 10.

Dynamical Latent Heat

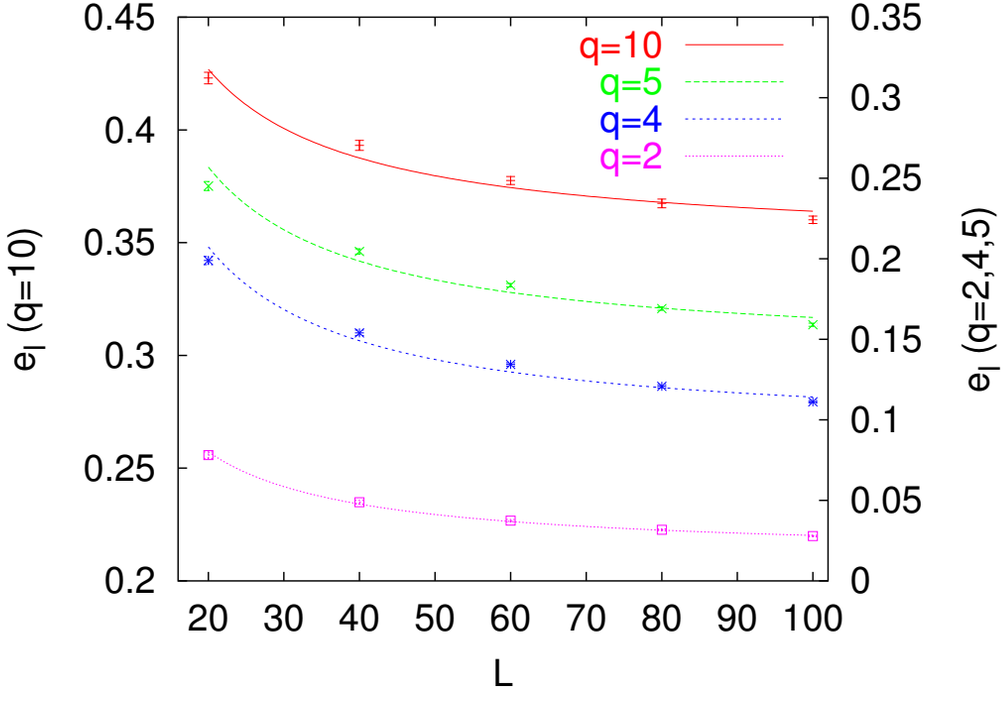

Figure 4: Latent heat estimates from hysteresis curves $\Delta e_l(L) = \overline{\Delta e_l} + \frac{a_1}{L}$. Heat-bath ($n_\beta = 1$).

The method gives estimates of β_c comparable to equilibrium data.

q	β_c	α	$\triangle e_l$	$\beta_{\min}$	$\beta_{\max}$	$\overline{\triangle e_l}$
2	0.440687	0	0	0.2	1.0	0.0153 (07)
4	0.549306	2/3	0	0.2	1.0	0.0907 (11)
5	0.587179	1	0.031072	0.4	1.2	0.1402 (12)
10	0.713031	1	0.348025	0.4	1.2	0.3482 (16)

Table 1: The phase transition temperatures $\beta_c = 1/T_c$, the specific heat exponent α and the latent heats of selected q-state Potts models in two dimensions. For the latent heats the negative energy per link $\triangle e_l$ is given and $\overline{\triangle e_l}$ is a dynamical latent heat estimate from hysteresis cycles: $\geq$ equilibrium latent heat.

Other Observables

- stochastic cluster properties
  - volume, surface, gyration radius
  - maximum volume and surface
  - distribution of these quantities
- percolation
- structure function:
  $S(\vec{k},t) = \frac{1}{N_s^2} \sum_{q_0=0}^{q-1} \left\langle \left| \sum_{\vec{r}} \delta_{\sigma(\vec{r},t),q_0} \exp[i\vec{k}\vec{r}] \right|^2 \right\rangle - \delta_{\vec{k},0} \sum_{q_0} m_{q_0}^2,$
  where $m_{q_0} = \langle \delta_{\sigma(\vec{r},t),q_0} \rangle$

Scenarios of Phase Transitions

- *Nucleation* is an instability against finite amplitude, localized fluctuations. It is dominated by the growth of the largest clusters.
  - Has an activation barrier.
  - Metastability.
- *Spinodal decomposition* is an instability against infinitesimal amplitude, nonlocalized fluctuations.
  - No activation energy.
  - Unstable region.
  - Linear Cahn-Hilliard theory predicts an initial exponential growth of $S(\vec{k}, t)$.

Cluster Definition

- Geometric cluster: Percolation coincides with the phase transition in 2D, but not 3D. Percolation exponents differ from critical exponents in 2D and 3D.

- Fortuin-Kasteleyn (FK) clusters: complete correspondence of critical and percolation properties. The Ising and $Z(3)$ models are studied in the equilibrium by MC simulations (Fortunato and Satz (2001)).

  FK or stochastic clusters remove artificial correlation by introducing the bond probability

$$p = 1 - \exp(-J/kT). \tag{11}$$

2D Models
Largest Connected Cluster Surface $S_{\max}$

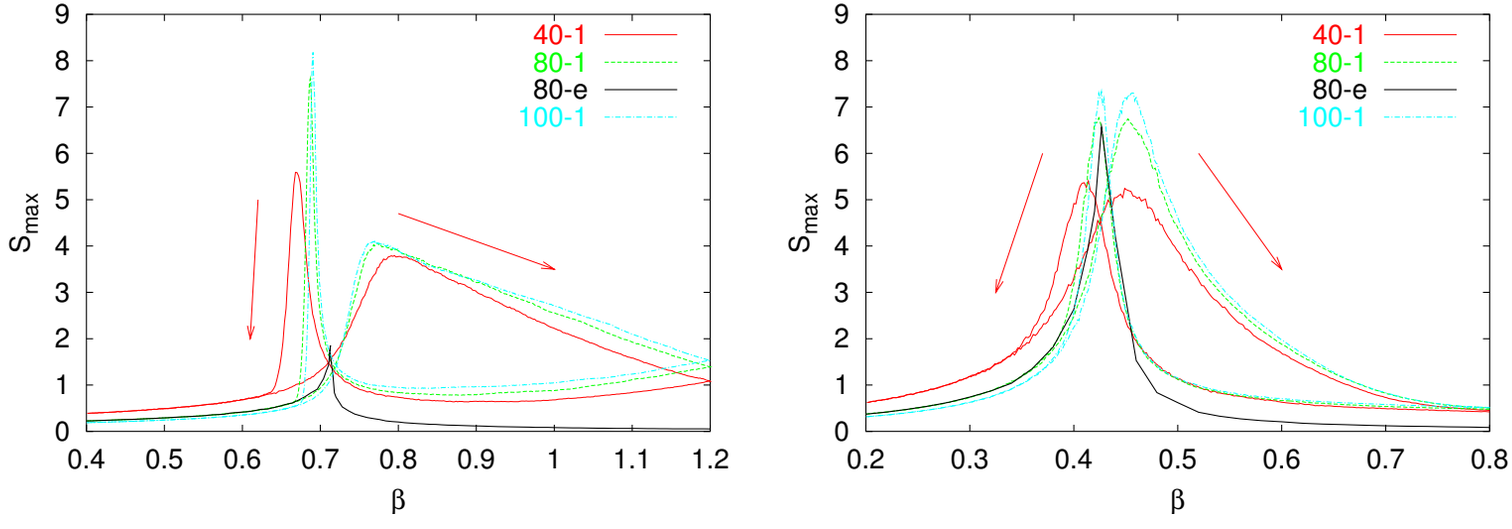

Figure 5: The largest cluster surface for the 10-state (left) and 2-state (right) Potts models.

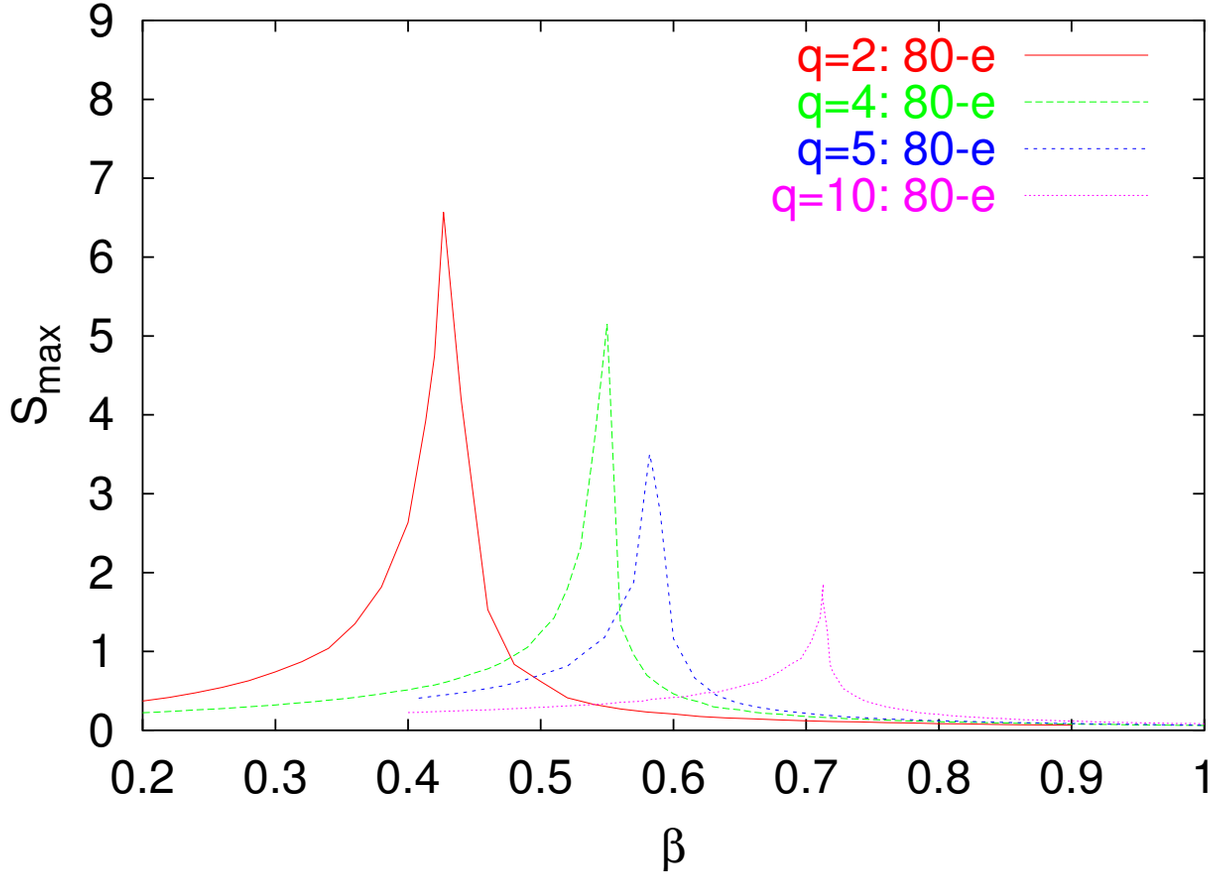

Figure 6: The largest connected cluster surface for equilibrium simulations. The strong 1st order transition does not favor the interfaces.

Percolation

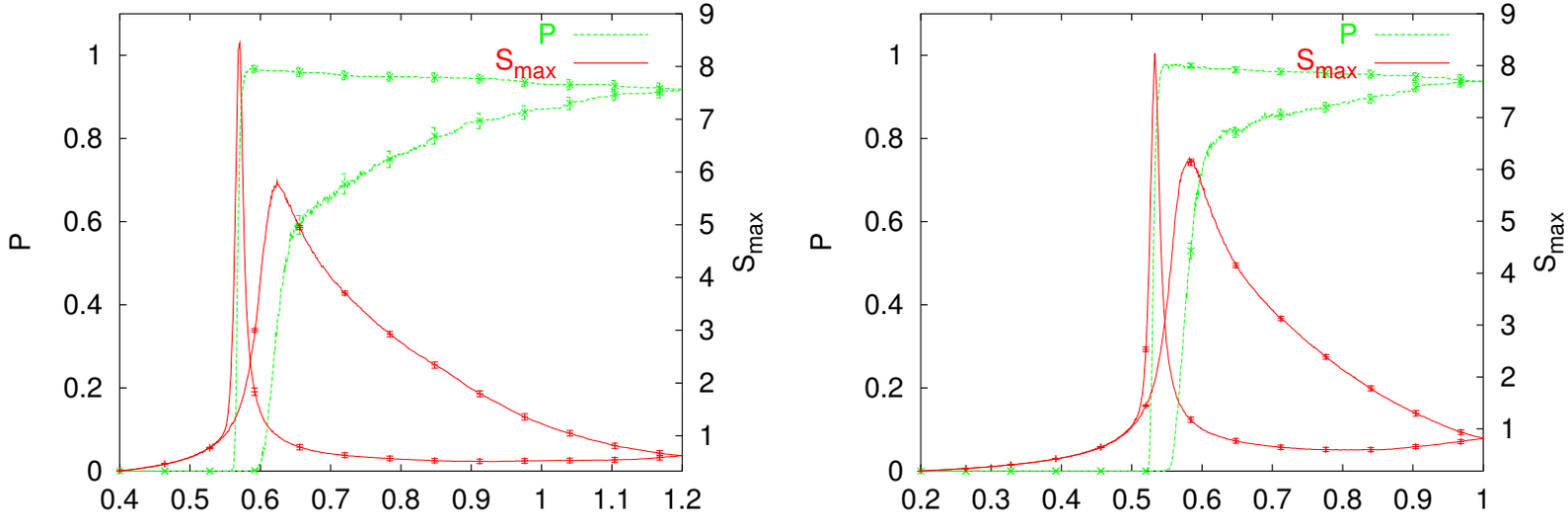

Figure 7: The percolation strength and the maximum surface; q=5,4 Potts models, L=100, $n_\beta = 1$

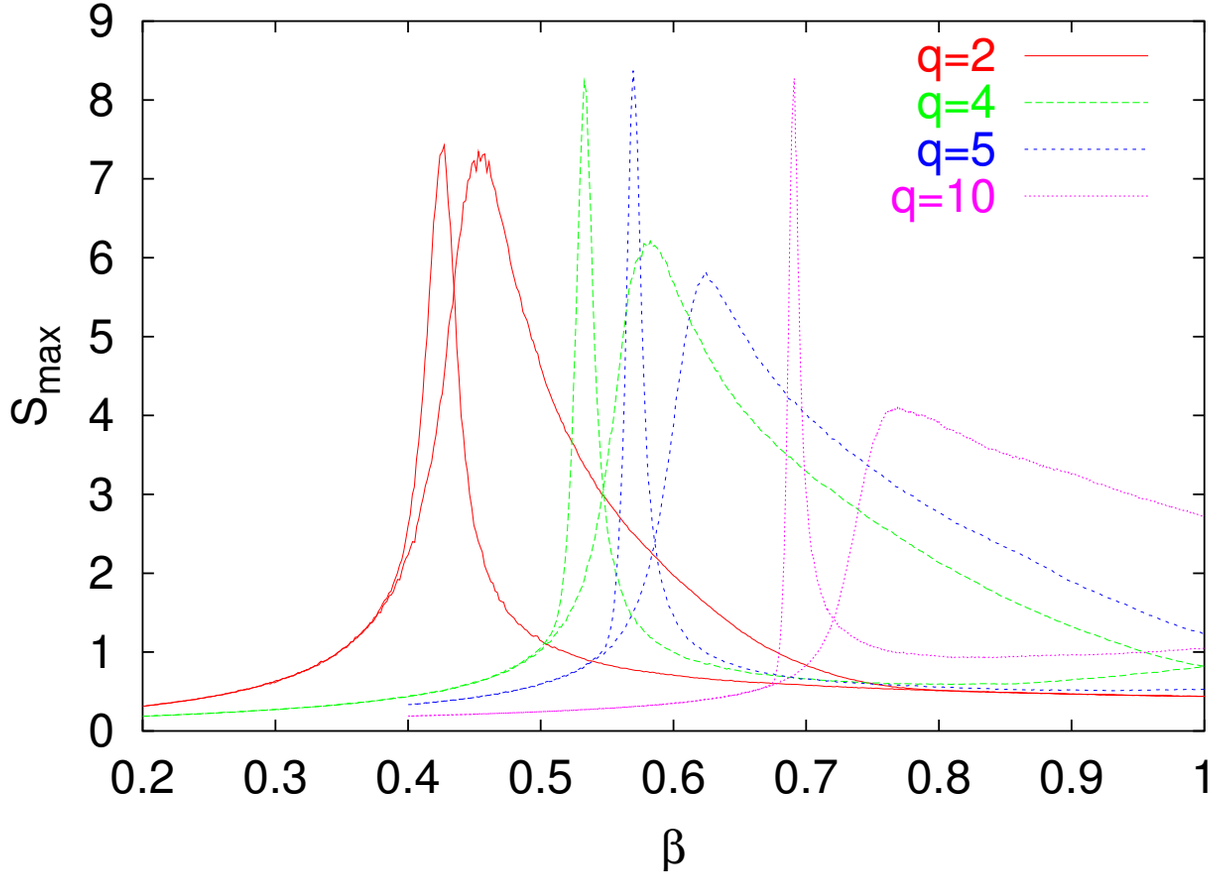

Figure 8: The largest cluster surface from dynamical simulations with $n_\beta = 1$ (100×100 lattices are shown).

Structure Functions

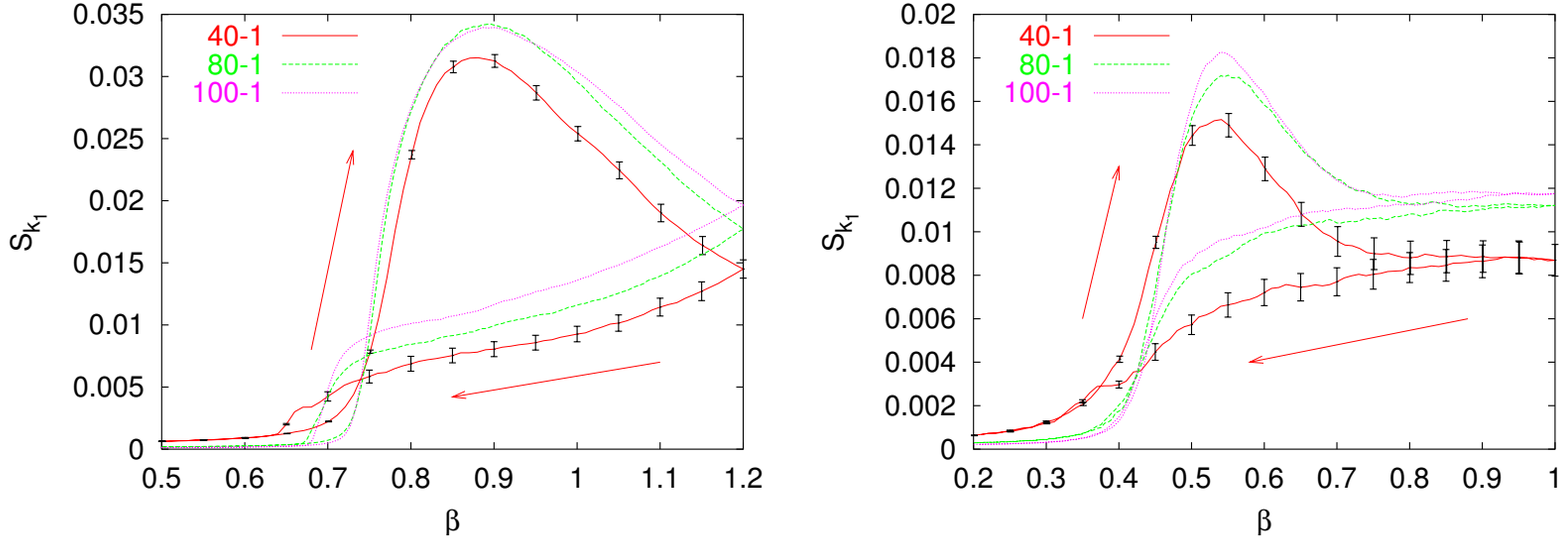

Figure 9: The structure function $S_{k_1}(\beta)$ for the 10-state (left) and 2-state (right) Potts models and fast (almost a quench) $n_\beta = 1$ dynamics. Large peaks are now only on the disorder $\rightarrow$ order (confinement $\rightarrow$ deconfinement) $\beta \rightarrow \beta_{\max}$ half-cycle. Equilibrium is not reached at $\beta_{\max}$

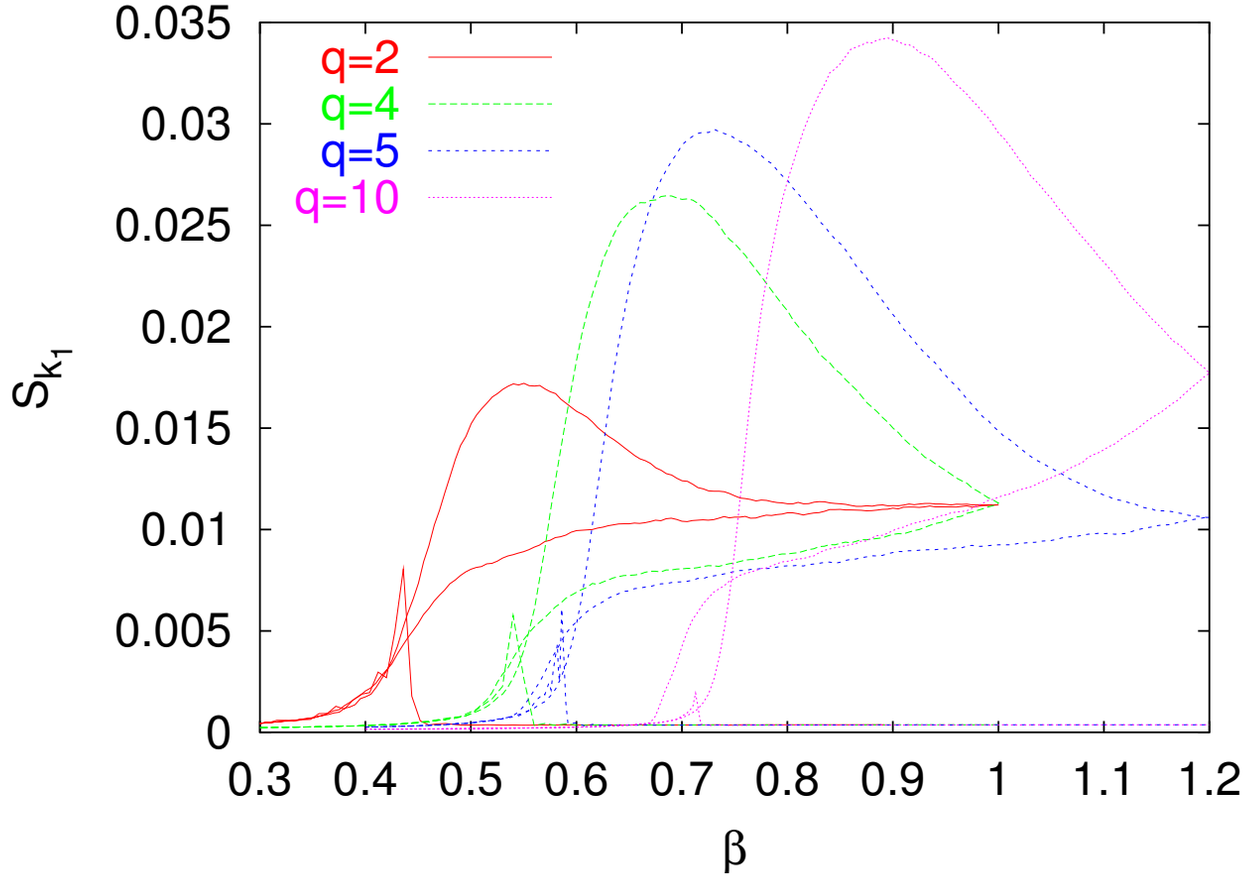

Figure 10: The structure function $S_{k_1}(\beta)$ from $n_\beta = 1$ dynamical simulations on 80^2 lattices together with their equilibrium values.

3-D 3-state Potts Model

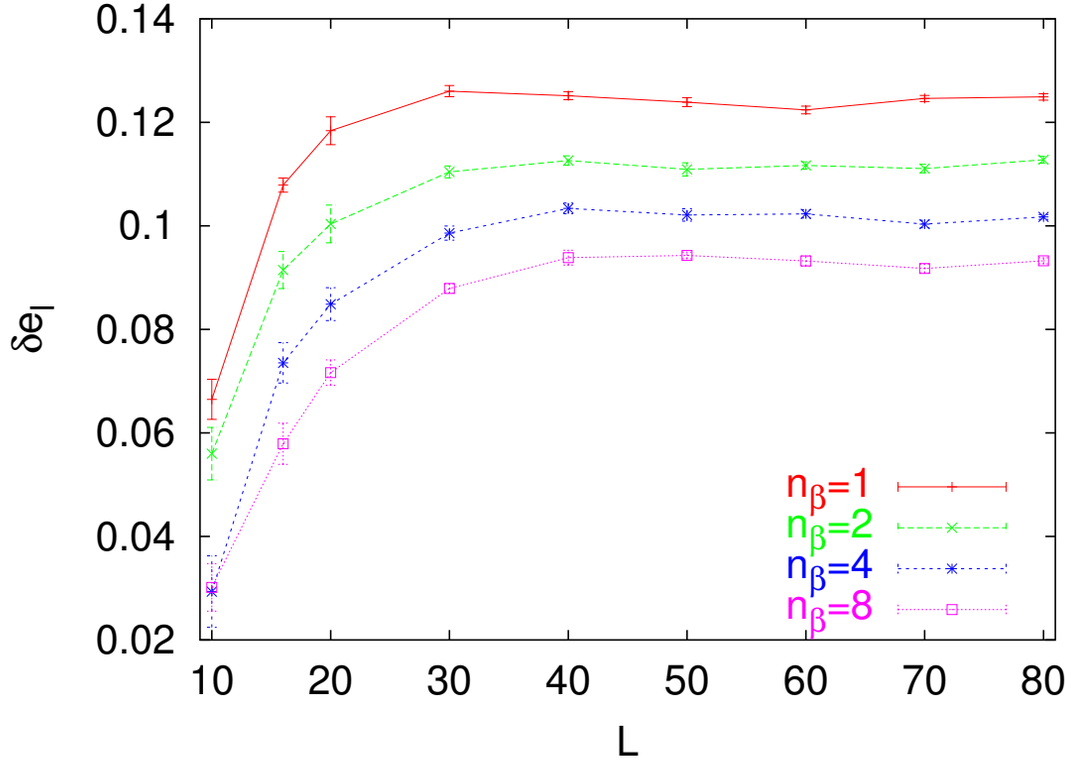

Figure 11: The finite size estimates of the latent heat for $n'_\beta = 1,\ 4,\ 8$ for the 3D 3-state Potts model at $h = 0$. The equilibrium value is $\overline{\Delta e_l} = 0.05354(17)$

Structure Functions – Quench

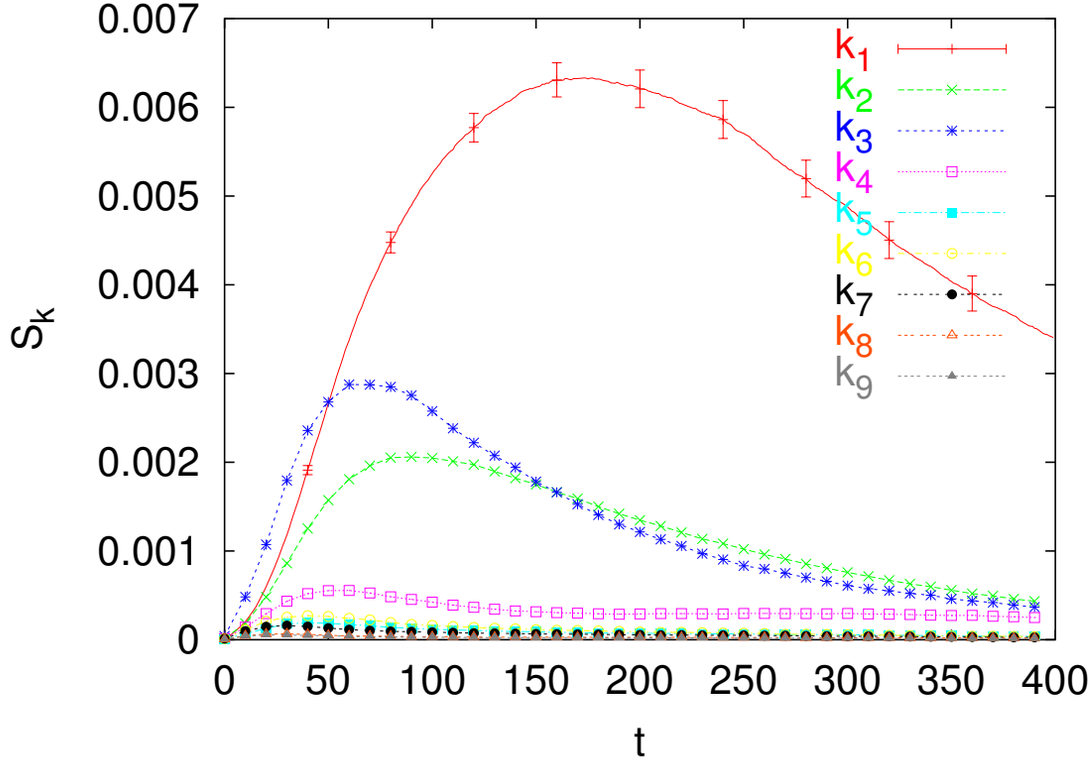

Figure 12: Structure function S_k for the $\beta = 0.2 \rightarrow 0.3$ $3d$ 3-state Potts model quench at zero field on a 40^3 lattice.

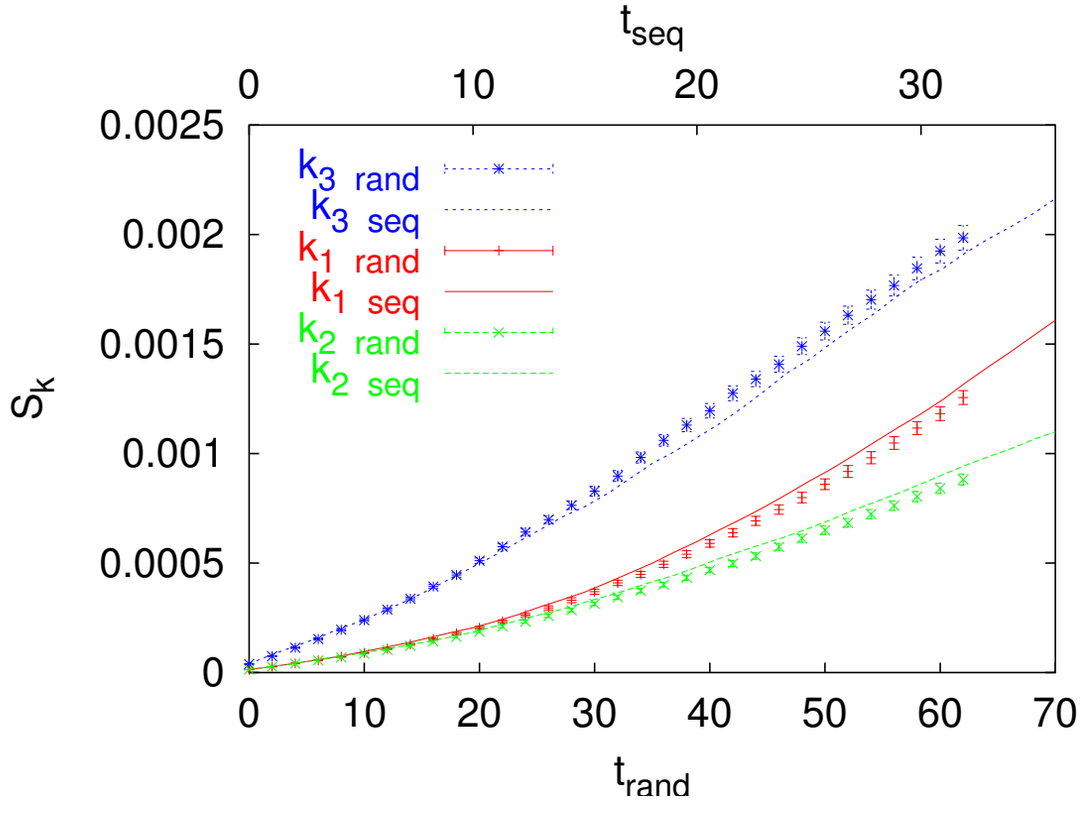

Figure 13: The early time evolution of the quench of the previous figure together with random updating data. The order in the legend agrees with the order of the curves.

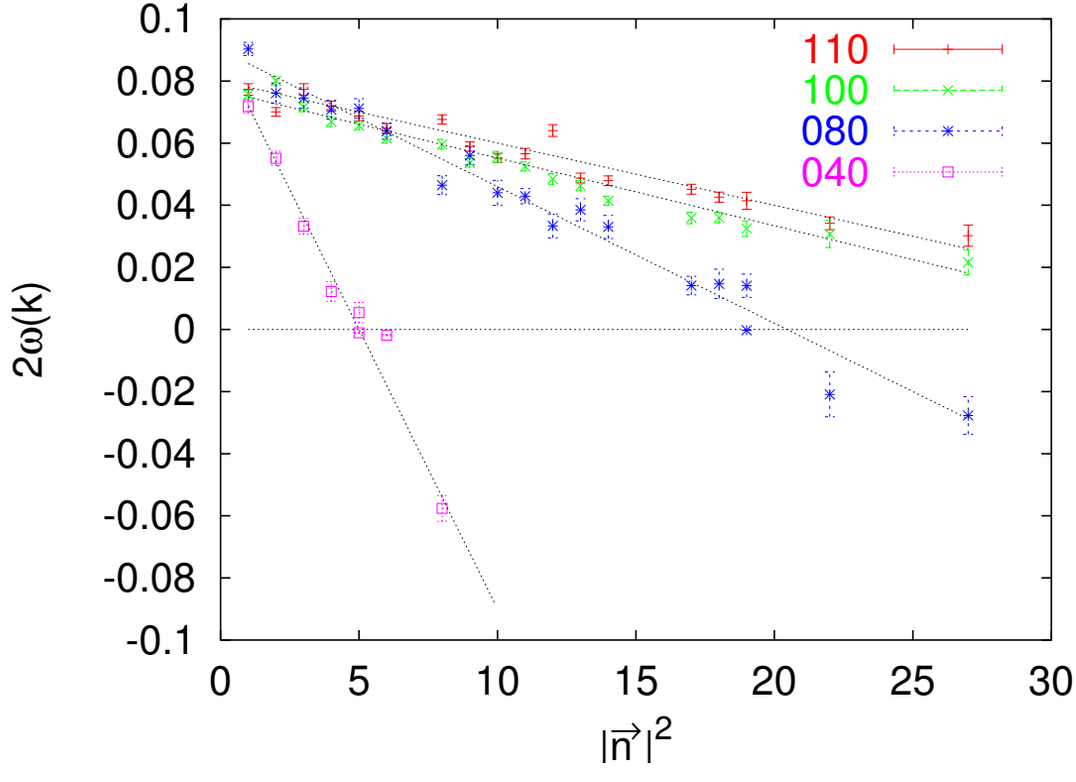

Figure 14: Determination of k_c for the 3D Potts model at zero field: $k_c \approx k_5 = 0.351$ $(L = 40)$ and $k_c \approx k_{16} = 0.342$ $(L = 80)$. Further, $|\vec{n}_c|^2 \geq 31$ for $L = 100$, 110.

Structure Functions – Hysteresis

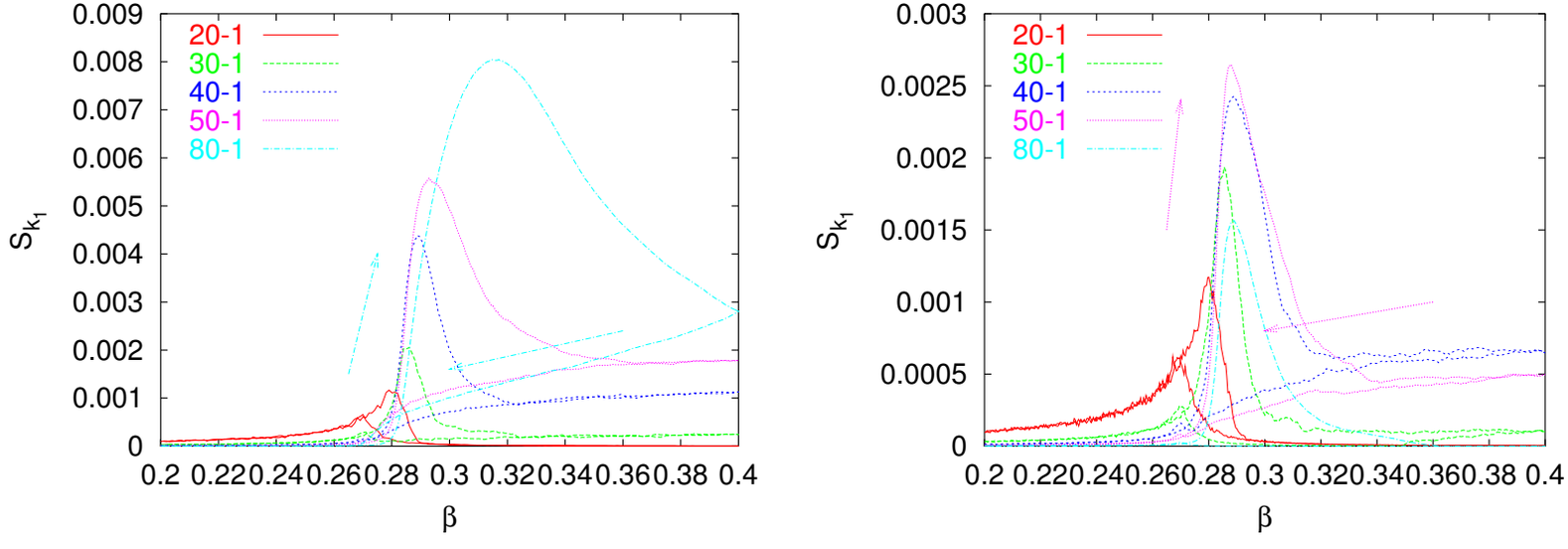

Figure 15: The structure function $S_{k_1}(\beta)$ for the $3d$ 3-state Potts model hysteresis in zero (left) and $h = 0.0005$ (right) external magnetic field.

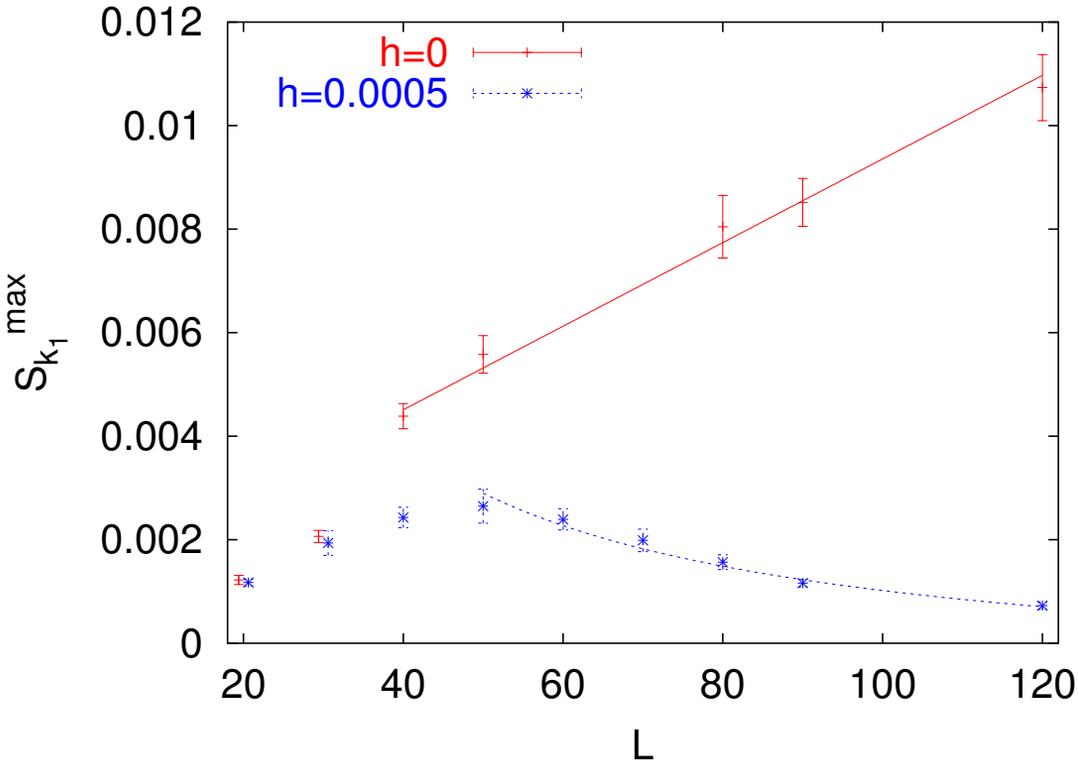

Figure 16: Structure function S_{k_1} maxima versus lattice size for the $n'_\beta = 1$ dynamics of the 3D 3-state Potts model without an external magnetic field ($h = 0$) and in the cross-over region ($h = 0.0005$). Asymptotic fits $a_1 + a_2 L^x$ with exponents $x = 1$ ($h = 0$) and $x = -1$ ($h = 0.0005$) are consistent.

Evolution of Largest Domains – Quench

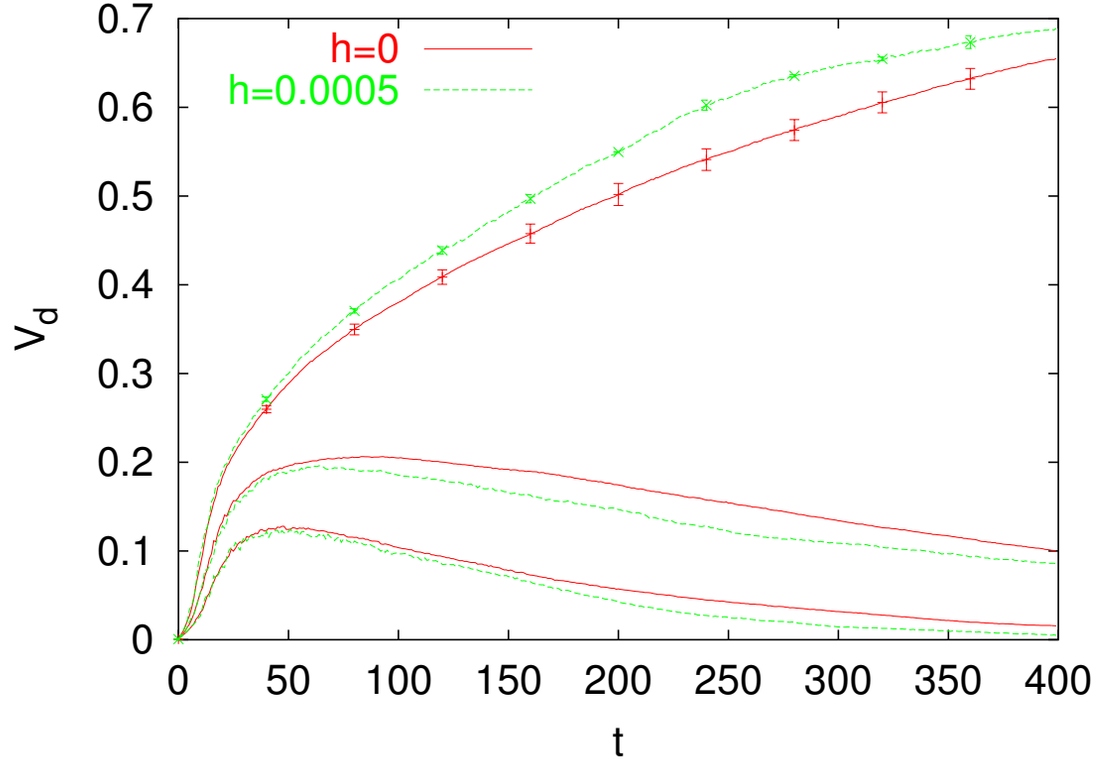

Figure 17: Time evolution of the largest domains of each of the trialities. Quench $\beta = 0.2 \rightarrow 0.3$ at $h = 0$ and $h = 0.0005$.

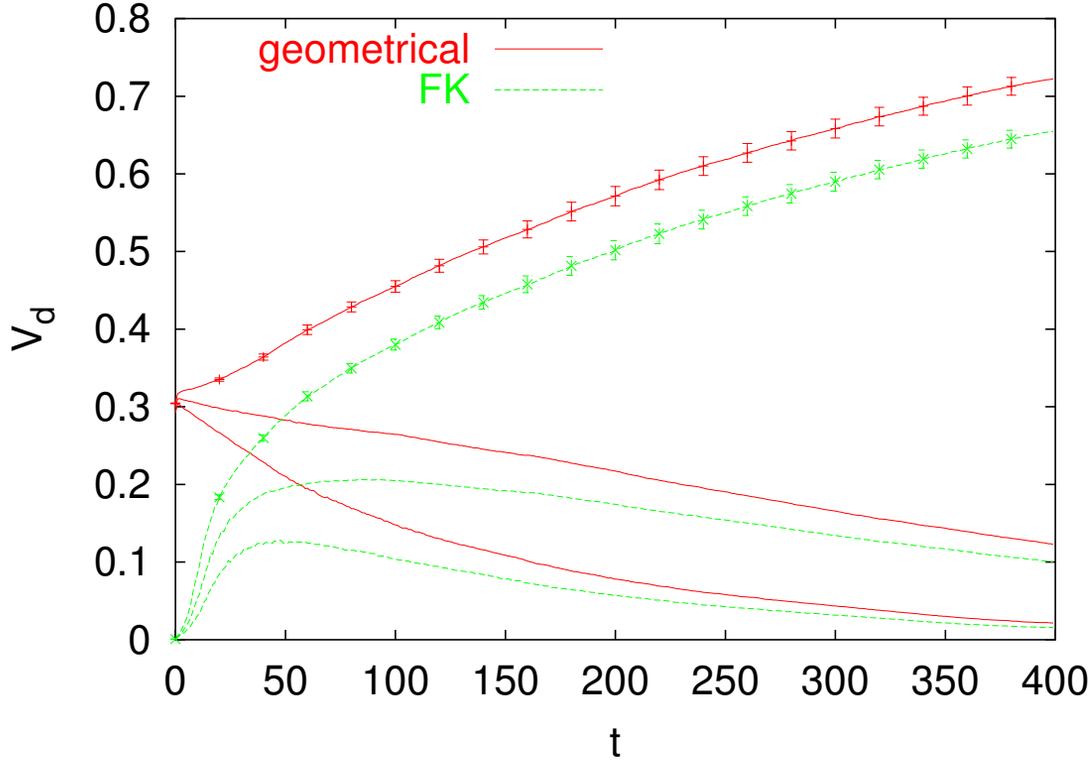

Figure 18: Geometrical and FK domains of the $3d$ 3-state Potts model quenched from $\beta = 0.2$ to $\beta_f = 0.3$ on a 40^3 lattice.

Summary and Conclusions

- Hysteresis effects may create a dynamical latent heat for 2nd order phase transitions.
- FK clusters give insight into the dynamics of the transition.
  - S_{max} is sensitive to the dynamics and related to the percolation of clusters. The $L \to \infty$ limit is not (yet) under control.
  - Domains of different trialities can prevent equilibration in the ordered phase
- Structure function allows to identify the transition scenario. We conclude that the transition from the disordered to the ordered phase proceeds by spinodal decomposition.
- Dynamics effects in our models are strong. Interfaces between domain may leed to an enhancement of low energy gluons.